Journal of Hydraulic Structures
J. Hydraul. Struct., 2022; 8(3):88-107
DOI: 10.22055/jhs.2023.41488.1223

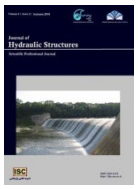

OPEN ACCESS

Simulation of Ogee Spillway by FLOW3D Software (Case Study: Shahid Abbaspour Dam)

Mohammad Amin Gandomi [1]
Mohsen Solimani Babarsad [2]
Mohammad Hosein Poormohammadi[1]
Hosein Ghorbanizadeh Kharrazi[1]
Ehsan Derikvand[3]

Abstract

Dam's weir is one of the most important dam structures that play a significant role in flood routing in the dam reservoir. Since the dam's level significantly affects the storage, changing the level and increasing its height can increase storage volume and flood control in some situations. Shahid Abbaspour Dam (Karoon 1), due to the reduction of the dam volume, affected by the accumulation of sediments and the construction of upstream reservoir dams, it is necessary to increase the dam's weir height. This research used a numerical simulation of the weir with Flow3D software. Moreover finally, after the model verification, its height was increased. All model outputs were compared with the physical model results and the dam's data, and the simulation fit well with both systems. According to the model results, in exchange for changing the level of the dam from 510 to 513.5 and the fully opening of the Gates, no negative pressure is created on the weir surface, and the cavitation index is within the allowable range.

Keywords: Dam, Ogee spillway, flood control, Flow3D, Karoon 1.

Received: 07 August 2022; Accepted: 28 October 2022

1. Introduction

Designed by the Harza Engineering Company in 1969, Shahid Abbaspour Dam (also known as Karoon-1) Dam was operationalized to achieve several purposes, such as providing hydroelectricity, meeting the agricultural demands of Khuzestan plains, and controlling the floods of the Karoon River. With a high generating capacity, this dam is one of the Iranian largest dams,

[1] Department of Civil Engineering, Water Resources Engineering and Management, Shoushtar Branch, Islamic Azad University, Shoushtar, Iran.
[2] Department of Water Sciences, Water Science and Environmental Research Center, Shoushtar Branch, Islamic Azad University, Shoushtar, Iran. Email: Mohsen.solb@gmail.com **(Corresponding Author)**
[3] Department of Water Sciences, Water Science and Environmental Research Center, Shoushtar Branch, Islamic Azad University, Shoushtar, Iran.

with a total capacity of 2000 MW. Upstream of Shahid Abbaspour Dam, two large dams, namely, Karoon-3 and Karoon-4, positively affect the possibility of controlling the floods, regulating the streamflow entering the dam's reservoir, and giving enough time to take preventive actions to reduce the reservoir level. Accordingly, the need to maintain the current 9.5 m freeboard over the normal weir level is discussed; however, considering the controlling effect of Karoon-3 and Karoon-4 dams, the floods entering the reservoir of Karoon-1 are still high and similar to the initial conditions. Therefore, experts seek to increase the weir level. It is necessary to make the design floods pass safely, control the level according to the latest regulations, and impose minimal change and cost to the dam. In other words, it is desired to reach the weir crest level of between 510 to 513.5 m above sea level. The normal level also increases to 536 and 538 m, respectively. The implementation of numerical models is currently one of the best options for engineers to design complex hydraulic structures. In recent years, numerous reports and articles have been published on the high precision of these models. For example Parsaie et al., [1] , Pirzad et al., [2] , Aein et al., [3] , Yildiz et al., [4] , Rajaa and Kamela, [5] , Ghazi et al., [6] , Morovati and Eghbalzadeh, [7] , Parsaie et al., [8] in a numerical study of effective parameters on hydraulic flows in proportional labyrinth weirs, Daneshfaraz et al. [9] ,Dehdar-Behbahani and Parsaie, [10] , Parsaie et al.,[11] , used FLOW-3D Software to investigate specific hydraulic parameters such as velocity distribution and vectors, fluid pressure distribution in the channel and weir, the Froude number, the stage-discharge curve and the discharge coefficient of labyrinth weirs with angles of 37˚, 42˚, 47.2˚ and 53˚ and a discharge rate ranging from 2 to 9 l/s. In this study, due to low values of relative and absolute error percentages, the RNG turbulence model was selected compared to LES, k-ε, and k-ω turbulence models. The results showed that with the same water head, as the angle increases, the flow rate and the Froude number decrease, and as the water head rises above the crest, the Froude number increases. Zamiri et al. [12] used the FLOW-3D used and previous research works to simulate a labyrinth weir with a sidewall angle of 6°. First, using three turbulence models (the k-ε, RNG k-ε, and LES models) in the FLOW-3D Software and previous research works, they simulated the weir model. The results showed that for a given discharge flow, the weir with an angle of 85° has the greatest Discharge, and the discharge coefficient increases as the sidewall angle values rise. They also suggested that the discharge coefficients of two weirs with angles of 85° and 55° were 2.28 and 1.24 times on average greater than the discharge coefficient of a weir with an angle of 6°. Setyandito et al. [13] investigated the flow characteristics of a trapezoidal weir using FLOW-3D with the Froude Number ranging from 0.051 to 4.367 in velocities between 0.055 m/s to 1.407m/s and three different slopes of 3V:1H, 3V:1H and 4V:1H for each model, respectively. The results showed that the Froude number is proportional to the average velocity and depth because the Froude number increases with an increase in the average velocity. However, the Froude number decreases slightly in a trapezoidal weir, but it increases downstream. Eventually, the model corresponds with the typical flow over the sharp-crested weir. In their research on a semi-analytical solution and numerical simulation of the water surface profile along a duckbill weir, Tajari et al. [14] solved the spatially varied flow equation. They obtained the water surface profile of a duckbill weir while bottom slots were used along the weir. In addition, FLOW-3D Software was applied to simulate the water surface profile along the weir. According to the results, the water surface profile along the weir calculated by the spatially varied flow equation and FLOW-3D Software is close to the experimental results, and the maximum calculation errors for the water surface profile were determined as 6.8 and 3.05 for solving the spatially varied flow equation and FLOW-3D Software, respectively. Shen and Zhang [15] conducted the 3D simulation of a carding weir with granular mixtures. The numerical simulation using experimental data by FLOW-3D Software showed that the simulation results of the flow

velocity, flow distribution, and the failure of the weir are in good agreement with the results from the physical model. Finally, the numerical analysis of hydraulic parameters and characteristics can provide technical support for future research on ecological weirs. In this regard, FLOW-3D is one of the most popular models in recent decades, capable of simulating complex geometries, including various types of turbulence and boundary conditions. The present study aims to adjust the weir level of Shahid Abbaspour Dam to increase the flood control level. Since the ogee shape of the weir is significantly influential in directing the flow over the weir toward the chute and on the energy dissipation system, the ogee shape of the weir should be modified following the changes in its crest level. Therefore, the present study analyzes and investigates the case of increasing the crest height of an ogee weir using numerical modelling by FLOW-3D Software and flow conditions.

2. Materials and Methods

Shahid Abbaspour Dam is located 135 kilometers northeast of Ahvaz and 50 kilometers east of Masjed Soleyman over the Karoon River. Fig. 1 shows the arch body, the weir approach channel, the weir body, and the downstream dissipator of the weir in Shahid Abbaspour Dam. The discharging capacity of the flow over the weir can be increased by adjusting the geometrical characteristics of the ogee weir. The significance of the modified geometry plan for weirs lies in the fact that for given water surface height, modifying the geometry of a weir increases the Discharge over the weir upstream [16].

2.1. Flow Equations

FLOW-3D Software discretizes the Navier-Stokes and continuity equations to simulate the flow, converting these partial differential equations to algebraic ones. Equations (1) and (2) represent the continuity and Navier-Stokes equations [17], respectively Where u_i, u_j, and u_k are components of velocity at the vertices i, j, and k, respectively, B_i is the volume force at the vertex i, μ is the dynamic fluid viscosity, ρ is the specific weight of water, x_i, x_j, and x_k are the coordinates at the vertices i, j, and k, respectively, and δ_{ij} is the Kronecker delta which is equal to 1 if i = j, and 0 otherwise.

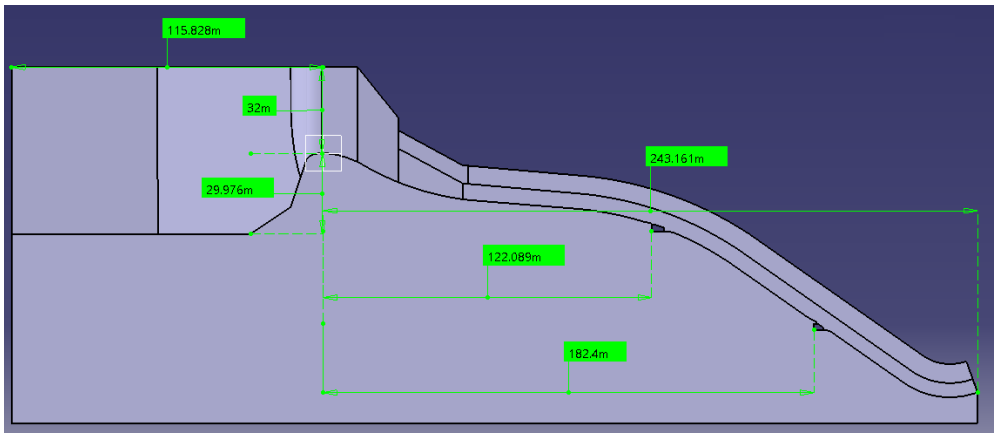

Figure 1. The aerial image of the body and weir in Shahid Abbaspour Dam

$$\frac{\partial \rho}{\partial t} + \frac{\partial}{\partial x_i} c = 0 \quad (1)$$

$$\rho\left(\frac{\partial u_i}{\partial t}+u_j\frac{\partial u_i}{\partial x_i}\right)=-\frac{\partial p}{\partial x_j}+B_i+\frac{\partial}{\partial x_j}\left[\mu\left(\frac{\partial u_i}{\partial x_i}+\frac{\partial u_j}{\partial x_i}-\frac{2}{3}\delta_{ij}\frac{\partial u_k}{\partial x_k}\right)\right] \quad (2)$$

2.2. Numerical Solution Characteristics, Solution Region, Turbulence Model, and Boundary Conditions

Using FLOW-3D Software, the present study simulates and investigates the effect of geometrical parameters such as the shape of weir crest, the approach channel to the weir, aerators, sidewalls, and middle walls. For this purpose, experimental and field data were used to conduct the verification process. In the present study, CATIA Software is used to define the geometry of solid body boundaries, and FLOW-3D Software is used to solve flow equations. Reynolds Averaged Navier-Stokes (RANS) equations present the equations governing the viscous fluid flow under turbulence are presented by Reynolds Averaged Navier-Stokes (RANS) equations. Since the weir flow is always turbulent, Reynolds equations are used in this modelling with the two-equation turbulence model to solve the turbulence flow and calculate the turbulence stresses (Reynolds stresses) for computational purposes. The present study uses a modified version of the standard k-ε model, namely, the RNG k-ε model, which is extracted from the normalization of Navier-Stokes equations using a robust statistical tool, i.e., the RNG method. Considering previous research, including [18,19]. The authors selected this model due to its reliability in answering various problems, accurate equation solving, high precision in showing flow details, and good performance in simulating flow separation regions and curvature of streamlines.

Table 1. Hydraulic and geometric characteristics of the models in this study

Initial Crest ELV. (m)	Proposed crest ELV. (m)	Discharge (m^3/sec)	Weir length (m)	Weir width (m)
510	512.5	3000-15000	243.161	54

2.3. Free-Surface Flow Modeling

In order to determine the free surface, several methods are used, which are different from the approach to solving the flow field [12]. The Eulerian approach to flow is used to determine the free surface in the flow field with a fixed grid. The present study applies the volume of fluid (VOF) Model to obtain the free surface [20]. A differential equation is solved for each cell volume fraction, and eventually, the fluid volume fraction value is determined for each cell. The 2D form of this differential function is as follows:

$$\frac{\partial F}{\partial t}+u\frac{\partial F}{\partial x}+v\frac{\partial F}{\partial y}=0 \quad (3)$$

In solving the above equation, F is equal to 1 in a fluid-filled cell while it is equal to 0 in a fluid-free cell. The value for F is between 0 and 1 in a surface cell. When Navier-Stoke and VOF equations are applied, parameters of viscosity and specific weight of the fluid are determined for each cell according to the following relations, and a combination of two fluid phases is seen in terms of the density and viscosity of each cell (Fverify the accuracy of the software results, a 2D bar model of the entire path of the weir from the reservoir to the ski-jump bucket was developed. This modelling aimed to investigate the boundary conditions and provide a qualitative observation of the results, including the flow pattern, velocity distribution, pressure, and flow status over aerators. In this modelling, the dimensions of the prototype were simulated at a scale of 1:1. A 2D

flow in the shape of a bar was assumed through the entire path of the weir without transversal flows in a way that the middle walls were not overflowed. In this simulation, 80m of the reservoir, the ogee and chute parts of the dam and up to the ski-jump bucket were modeled along with all the aerators. The simulation was conducted with the 532.5 m normal reservoir level and 100% gates opening. In addition, the width of the weir was assumed to be 80cm in the bar model. A single primary and four secondary mesh blocks were used to mesh the geometry and flow field. Fig. 2 shows the primary block that starts from the weir upstream and continues to the end of the ogee crest.

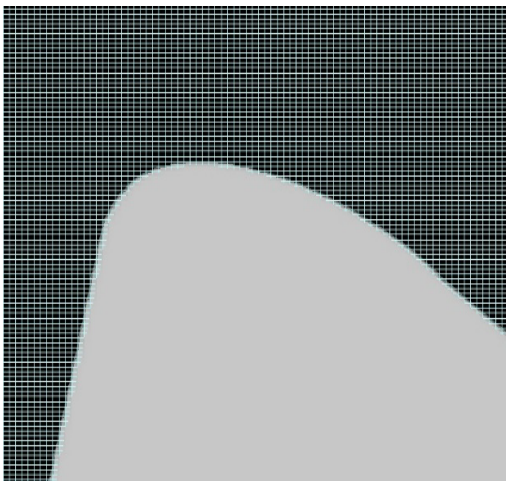

Figure 2. flow field Mesh of geometry

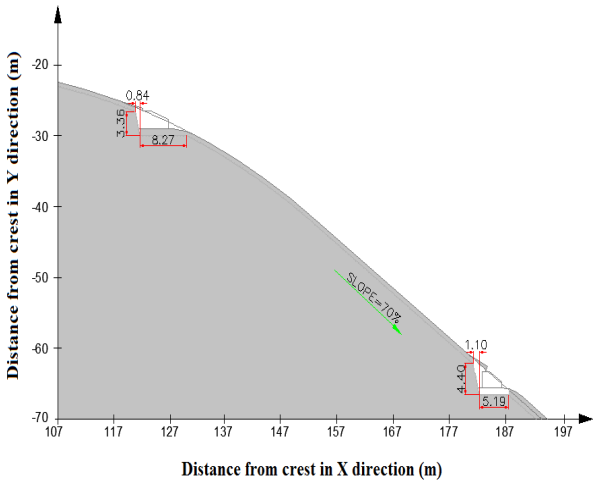

Figure 3. Aerator dimensions

According to these boundary conditions, the concrete roughness height (k) is considered to be between 0.1 and 3mm [21]. Therefore, in the bar model of the weir, the roughness height was considered to be 0.1mm (smooth concrete). As shown in Fig.3, the applied boundary conditions in the blocks include the symmetry boundary condition for a boundary on the lateral side of the bar. Table 2 shows the characteristics of the total time of calculation and mesh and block dimensions at the vertices X, Y, and Z.

Table 2. The model characteristics

Field Dimensions		
Along Z-axis (m)	Along Y-axis (m)	Along X-axis (m)
114	0.8	323
Final block meshing dimensions		
Along Z-axis (m)	Along Y-axis (m)	Along X-axis (m)
40	40	40
Total grid and time of calculation		
Total time of calculation (h)	Total number of calculation grids	Secondary blocks
72	925120	4000

A. Turbulence Modeling

As an influential factor in the time of calculating numerical models, turbulence simulation is a critical topic in fluid dynamics. Lack of fluctuation and change in the flow discharge at the weir outlet are among the solution stability criteria. As shown in Figs. 4 and 5, this is what happens 50

second after the solution is started. The results also imply equal input and output flow discharges. Accordingly, the mean turbulence energy and the mean kinetic energy are investigated. Figs. 6 and 7 show the results.

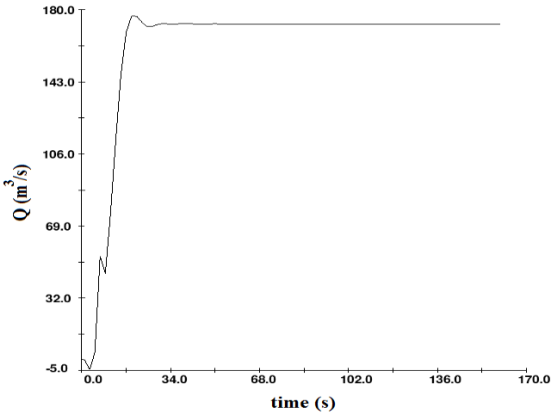

Figure 4. Input flow discharge of the solution field

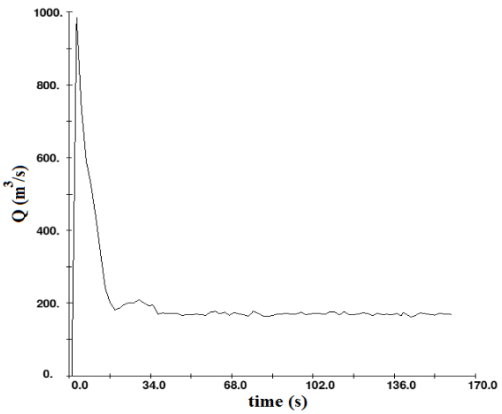

Figure 5. Output flow discharge of the solution field

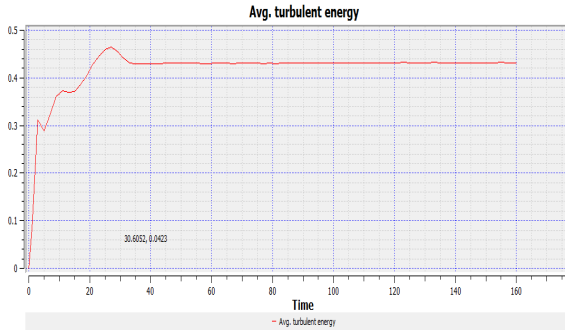

Figure 6. Stabilization of the mean turbulence energy

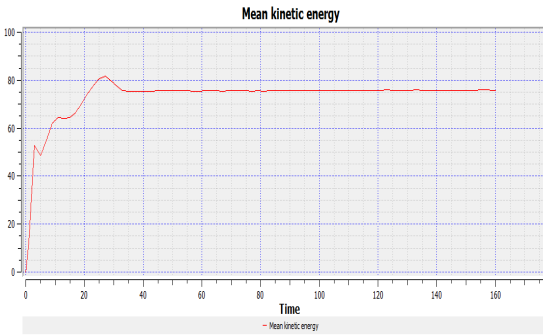

Figure 7. Stabilization of the mean kinetic energy

B. Weir 3D Modeling

The 3D model of the weir in this dam was investigated, and the results are provided here. This study aims to verify the numerical model according to the information of its physical model. In the present study, the already existing map and information were used to develop the numerical model for the weir of Shahid Abbaspour Dam (at the scale of 1:1). The reservoir topography was obtained using all the available information, including the existing images of the weir physical model in 1993. Figs. 8 and 9 illustrate the geometric characteristics of the spillway and the reservoir area. As the maximum depth of the apex over the weir reaches 30m during the maximum level, the effective area in the discharge coefficient of the weir is considered to be 50m of the dam's reservoir in the computational model, and the calculations regarded up to the level of the bottom of the weir approach channel.

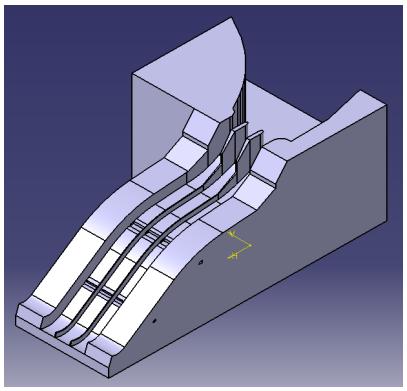

Figure 8. The total 3D area of the weir

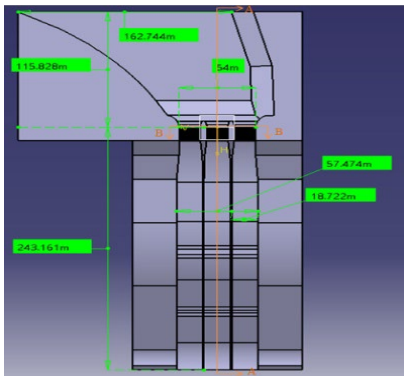

Figure 9. General plan as the simulator input

2.4. Boundary Conditions, Model Meshing, and Selection of the Weir 3D Turbulence Model

The model's geometry was outlined using CATIA Software. After the model's geometry was inserted in FLOW-3D, the modeling stages included initial settings for the model, meshing, introducing initial and boundary conditions, and eventually, implementing the model and presenting the results. Two uniform meshing blocks were used to mesh the solution field. The first block starts from 50m upstream of the weir crest inside the reservoir and finally ends at the weir crest. The second block starts from the weir crest and continues to 40m downstream of the crest, i.e., the ogee ending area. These two areas are shown in Fig. 11. This is why the model is divided into two segments. The stage-discharge curve, the distribution of pressures on the ogee, and the possibility of negative pressure were taken into account, and a wider area will not affect the results. In addition, there were too many calculation grids in the 3D modeling, and the solution time was significantly long. Therefore, modeling is conducted up to the end of the ogee to perform the verification studies for the stage-discharge curve. In order to assess the sensitivity of the model to the mesh, four meshing cases are considered for the model. Table 3 shows the characteristics of the model meshing. It should be noted that in all the figures of this section, the origin point is the location of the crest, and the weir lies at the midpoint of the crest's axis.

Table 3. Characteristics of the weir model meshing

The cell size for Case 1	Along X-axis (m)	Along Y-axis (m)	The cell size for Case 1
20	20	40	Case 1
40	10	40	Case 2
40	20	40	Case 3
80	40	80	Case 4

Figure 10 shows the amount of relative residual error statistics. according to this figure, the value at the end of the solution is less than 0.0025.

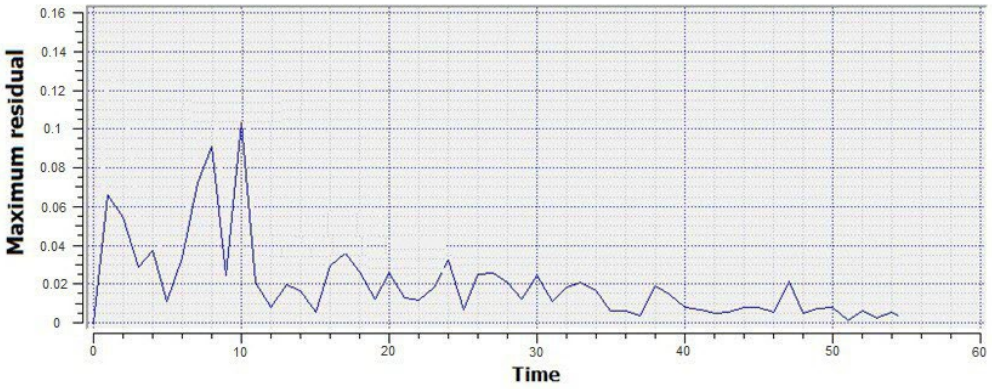

Figure 10. The amount of remaining error statistics

The fourth case is regarded as the selected case since the difference between the obtained stage-discharge curves for the 4 cases is less than 0.2%, and the fourth case has fewer grids and takes less time to implement compared to the other cases. In this case, the mesh includes a total of 1976000 computational cells. Considering the number of computational cells, it takes 192 h to implement the models in case of open gates. The boundary conditions in the inlet are applied for the specific pressure, i.e., the fluid level is applied in the inlet. Accordingly, under these boundary conditions, the water surface level in the reservoir is determined, and the flow discharge is obtained using the numerical model. The lateral boundaries and the model's bottom follow the boundary conditions of the wall using the wall function in node points near the boundary. In these boundary conditions, the concrete roughness height (k) is between 0.1 and 3mm. Table 4 compares the flow discharges obtained from the numerical model using various roughness values within the range above when the water level is 532.5 m in the reservoir, and the flow discharges obtained from St. Anthony Falls experimental results (Q = 10037 m3/s). As it can be seen, the results are not sensitive to roughness because the ogee path is a falling jet path, and there is less friction in the path. Therefore, there is little difference between the obtained values for discharge flows. It should be noted that Kim and Park, [22] also reported the insignificant effect of roughness on the flow over the ogee weir [22]. Fig. 12 shows the applied boundary conditions. At first, the entire solution space is filled with fluid, and as the solving process continues, the fluid is drained from the output boundary and reaches its final state.

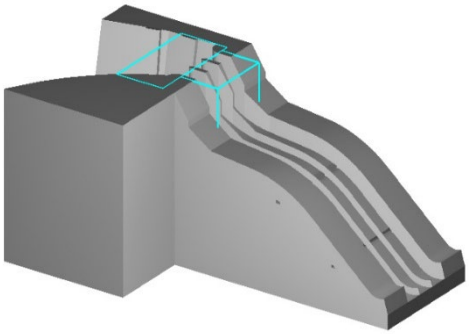

Figure 11. The 3D geometry of the weir plan and the modeling area using two blocks

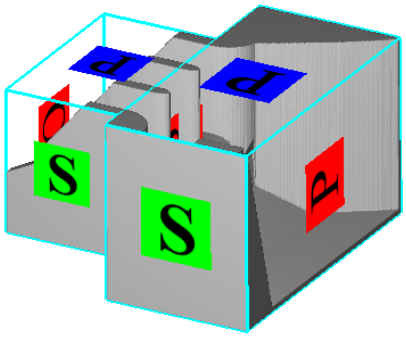

Figure 12. The boundary conditions applied to the solution field

Table 4. A comparison between the numerical results and the experimental results for the reservoir level and the weir crest

K (mm)	Q(m3/s)	Error (%)
0.1	10024.52	0.13
1.1	10013.61	0.23

3. Results and Discussions

3.1. Qualitative Evaluation of the Numerical Results from the Bar Model

In this section, the water head in the input boundary is considered to correspond with the level of 532.5m, or the current normal level of the reservoir. Figs. 13 and 14 show the velocity vectors and Fig. 15 illustrates how the flow passes over the weir. According to these figures, the pattern for the flow over the ogee weir and aerators is perfectly reasonable, and there is no flow separation along the weir. The free surface level of water reaches a point where the F coefficient changes the value from 1 to 0. Therefore, The F coefficient meter can show the location of the free surface. Fig. 16 shows the level lines of pressure along the weir. According to this figure, there has been no negative pressure at any flow point.

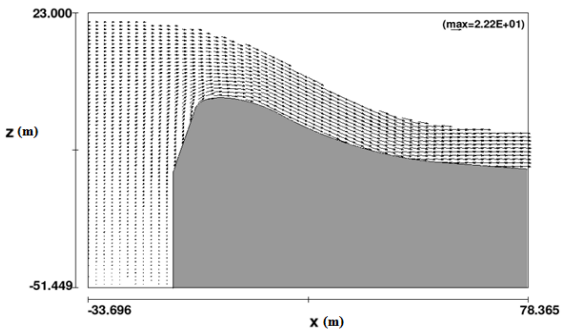

Figure 13. The velocity vectors in the ogee weir

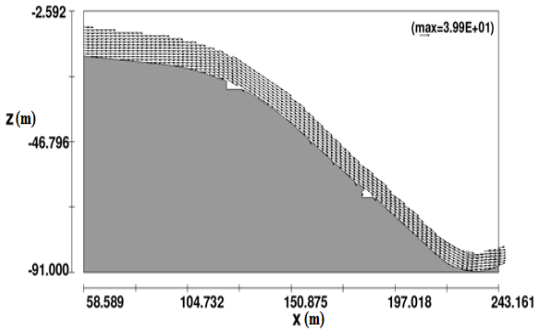

Figure 14. The velocity vectors in aerators and ski-jump bucket

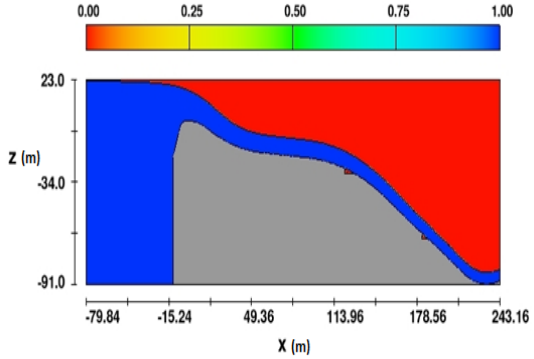

Figure 15. The level curve of volume fraction

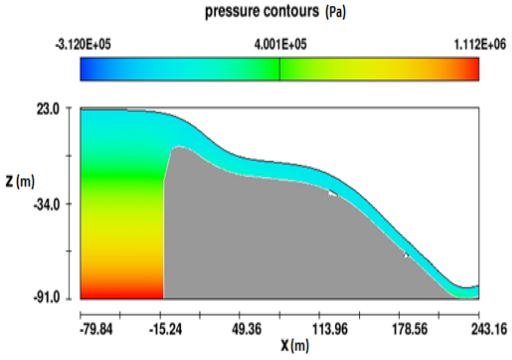

Figure 16. The level curve of pressure

Finally, in 0.8m along the weir and for the calculated flow by the model and over the weir, the discharge rate is 170 m^3/s. Accordingly, the weir inlet coefficient is obtained as 1.99, which is acceptably less than 5% different from the theoretical value of 2.1 and the experimental value of 2.05 (the report on the weir physical model) in the targeted head. After the upstream weir geometry

is completed, the weir 3D model is to be implemented to obtain the relationship between the free surface level of water, the weir discharge rate, and an increase in the weir level for the present situation.

3.2. Flow Analysis in Case of Fully-Open Weir (All Gates Open)

The present study simulated the conditions of fully-open gates and maximum reservoir level in PMF discharges according to the initial plan of the weir, i.e., 540m (the water head over the weir crest is 30m). The following figures show the obtained flow pattern, the water surface level, and calculated pressures along the path, including over the ogee part of the weir. Fig. 21 and Table 5 show the calculated pressure over the middle axis of the present ogee weir in the case of a full gate opening. According to this figure, no negative pressure is built up at the bottom of the ogee weir. As shown in the figure, when the level increases, which subsequently increases the discharge rate, there is a decrease in the pressures over the weir crest that follows a jet trajectory because when the discharge rates are high, the jet has a longer trajectory and takes more distance from the ogee curve. However, when the jet reaches the perpendicular and concave curve of the weir bed, the pressures increase due to a depth increase in higher discharge rates.

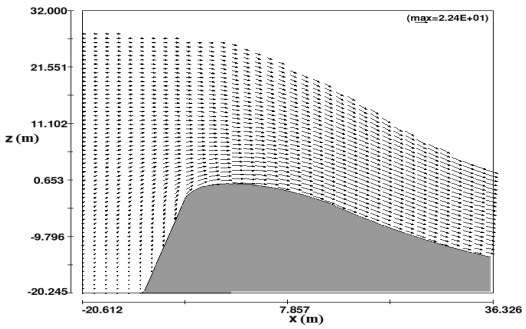

Figure 17. The general flow pattern over the weir in the 3D model with a reservoir level of 540m above sea level

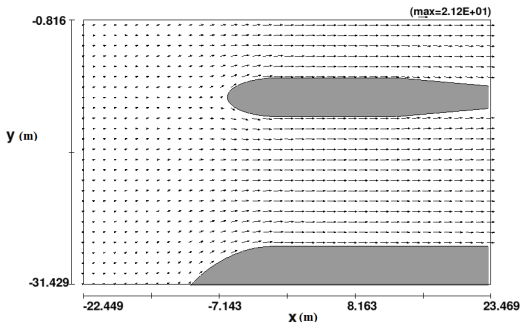

Figure 18. the flow pattern around the weir bases in the 3D model with a reservoir level of 540m above sea level

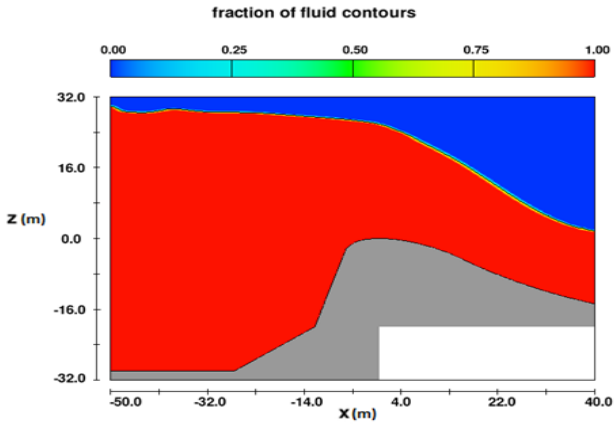

Figure 19. The calculated pressures in the 3D model with a reservoir level of 540m above sea level

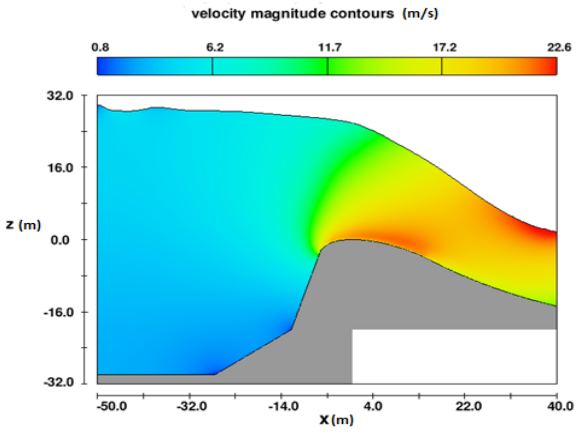

Figure 20. The calculated velocities in the 3D model with a reservoir level of 540m above sea level

A velocity contour was examined on the crest region to investigate the change in crest elevation (Fig. 20).

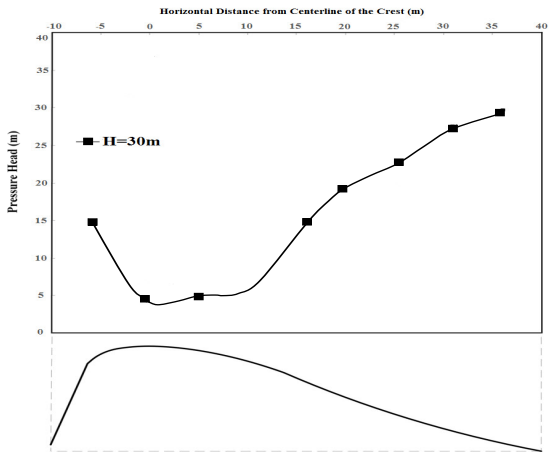

Figure 21. The profile of pressure over the middle axis of the present ogee (the full gate opening)

Table 5. Pressure over the middle axis of the present ogee weir for different reservoir levels in the case of the full gate opening

H=30 m	P (m)	14.74	4.39	4.77	6.13	14.91	19.26	22.77	27.48	29.61
	X (m)	-5.80	-0.60	5.00	10.60	16.20	19.80	25.40	31.00	36.20

3.3. Stage-Discharge Curve Comparing the Results

The FLOW-3D performance was verified using the data from the physical weir model presented in 1993 by a report from the Water Research Institute and the results from Harza Company and the St. Anthony Falls Laboratory. Considering fully open gates in various reservoir levels, Fig. 22 shows the difference between the numerical model results and the results presented by the Water Research Institute and Hazara Company. The data in this table shows that the results of the numerical model and the experimental curves presented by the St. Anthony Falls Laboratory

[8] are in good agreement in a way that in two cases, the difference is about 9%, while many other cases differ less than 1%. This fact indicates that the numerical model can simulate the flow over the weir in this study. It should be noted that the difference between the results of the numerical model and the physical weir model from the Water Research Institute is about 13% in case of maximum level and full gate opening.

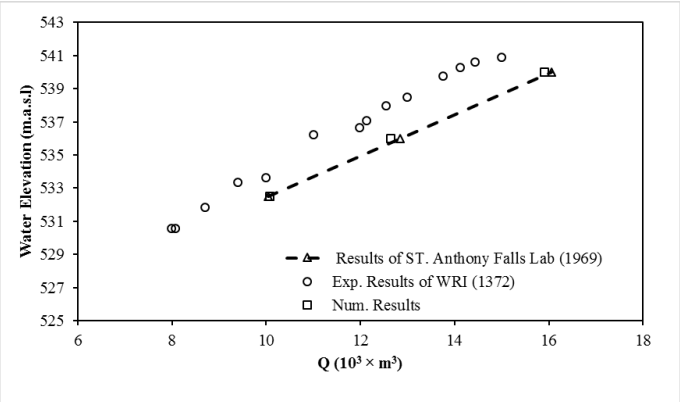

Figure 22. The stage-discharge of the weir in the case of the full gate opening

3.4. Comparing the Results for the pressure on the Bottom of the Ogee Weir

Fig. 23 shows the pressure on the bottom of the ogee weir in the numerical Model (the present study) and the experimental Pressure (the experimental results from the St. Anthony Falls Laboratory) in the discharge rate of 8000 m3/s and the full gate opening with already available information. As shown in Fig. 23, the numerical model can predict flow characteristics such as pressure. There is a maximum difference of 34% with the experimental results related to a point at a 12.6m distance from the weir crest. However, other points show an average difference of 11.3%. In this figure, the horizontal axis is the distance from the weir crest along the ogee segment, and the origin point is the location of the crest. The vertical axis shows the pressure on the crest (m). The figure also shows that the calculated pressures from the numerical model are less than the measured values. Therefore, it is a safety measure.

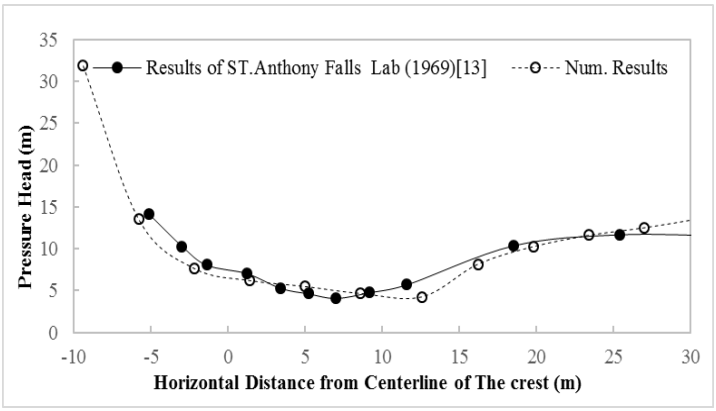

Figure 23. Comparing the numerical and experimental models for Q = 8000 m3/s and fully open gates.

3.5. The New Upgraded Numerical Model of the Weirs

The boundary conditions, turbulence model, mesh dimensions, and other input parameters of FLOW-3D are entirely similar in the new numerical model (with upgraded crest) and the 3D numerical model for the present weir. It should be noted that the geometry of the ogee crest is the only change in the new numerical model in which the crest level is changed from 510 to 513.5m above sea level. In this section, the results of the numerical model for the new weir are first investigated for different water levels of the reservoir and entirely gate opening. Then, the obtained results are analyzed and compared. In this case, only the geometric characteristics of the longitudinal profile of the weir are changed, according to Fig. 24.

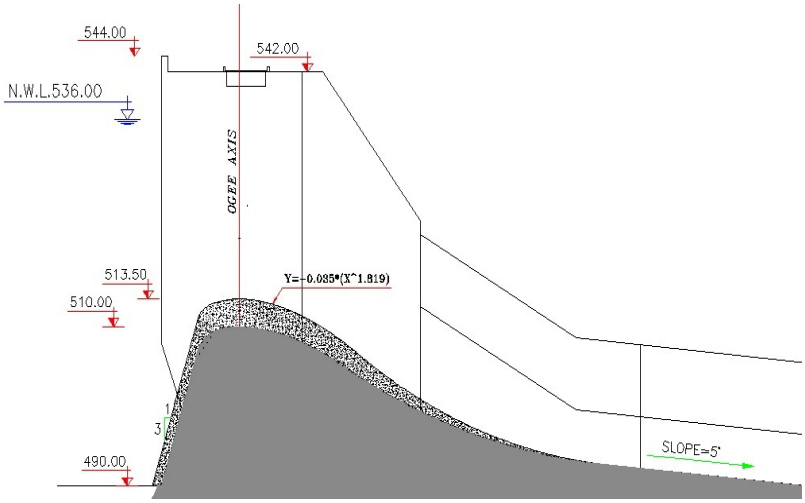

Figure 24. The new ogee profile with the ogee crest level of 513.5

3.6. Flow Simulation in the Case of Fully Open Weir (Fully Open Gates)

In the case of fully open gates, the water level over the weir (the same applied level for simulation of the present weir in the previous section) was applied, and the numerical model calculated the flow conditions and discharge flow. The level of 540m was obtained (the water head over the weir crest was 26.5m). The following figures show the flow pattern, the water surface level, and the calculated pressures along the path, including over the ogee weir. Fig. 30 and Table 6 show the calculated pressure over the middle axis of the ogee weir in the case of a complete gate opening. According to this figure, no negative pressure is built up at the bottom of the ogee weir. As shown in the figure, when the head increases, which subsequently increases the discharge rate, there is a decrease in the pressures over the weir crest that follows a jet trajectory because when the discharge rates are high, the jet has a longer trajectory and takes more distance from the ogee curve. However, when the jet reaches the perpendicular and concave curve of the weir bed, the pressures increase due to a depth increase in higher discharge rates.

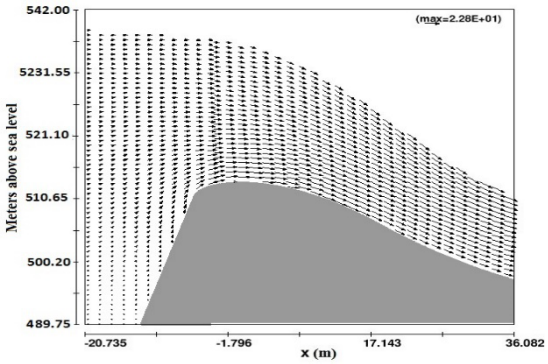

Figure 25. The general flow pattern over the weir in the 3D model with a reservoir level of 540m above sea level

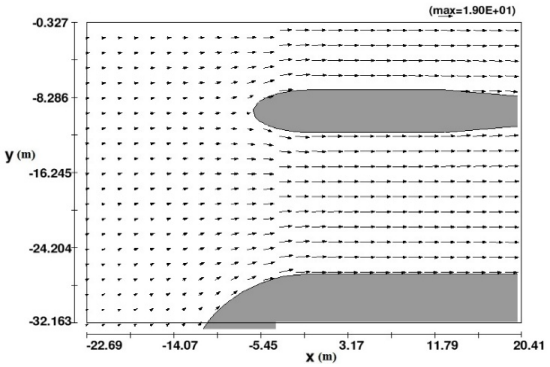

Figure 26. the flow pattern around the weir bases in the 3D model with a reservoir level of 540m above sea level

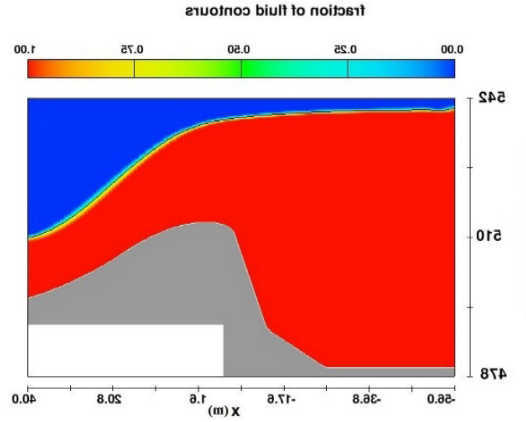

Figure 27. The calculated water surface level in the 3D model with a reservoir level of 540m above sea level

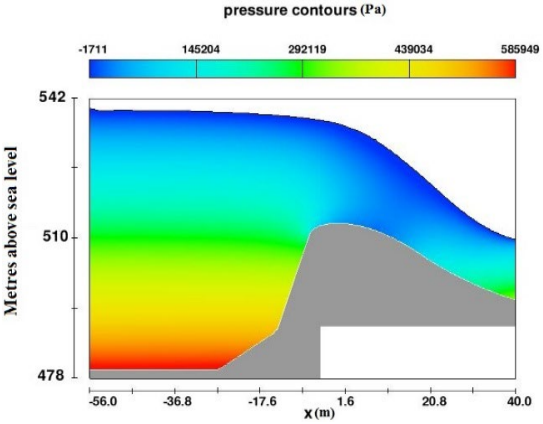

Figure 28. The calculated pressures in the 3D model with a reservoir level of 540m above sea level

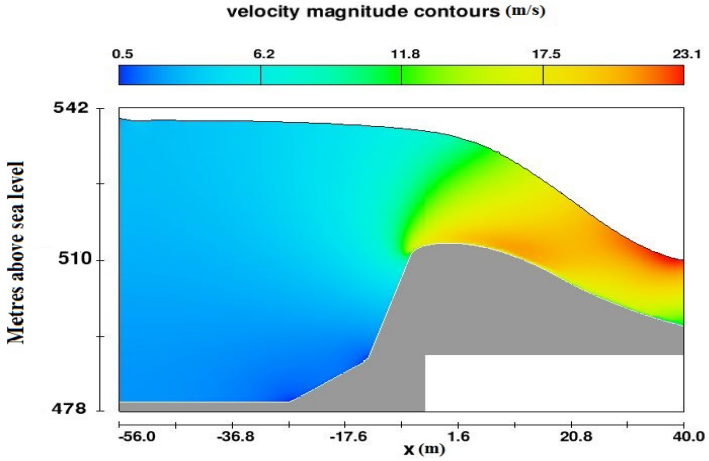

Figure 29. The calculated velocities in the 3D model with a reservoir level of 540m above sea level

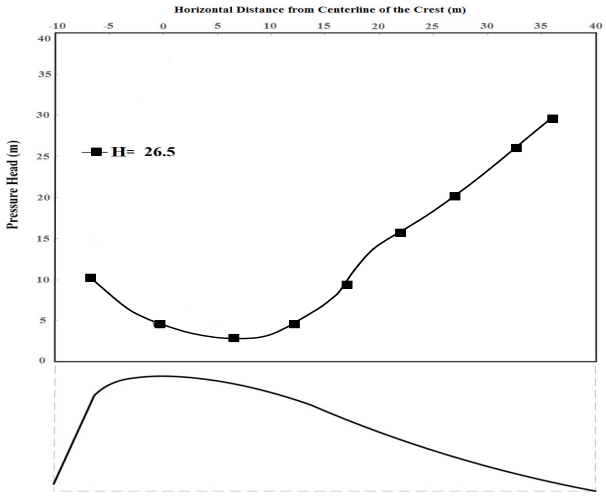

Figure 30. The profile of pressure over the middle axis of the ogee weir in the case of the full gate opening with the crest level of 513.5m

Table 6. Pressure over the middle axis of the ogee weir for the crest level of 513.5m

H=30 m	P (m)	14.74	4.39	4.77	6.13	14.91	19.26	22.77	27.48	29.61
	X (m)	-5.80	-0.60	5.00	10.60	16.20	19.80	25.40	31.00	36.20

Table 7 shows the discharge flow over a weir in the case of the full gate opening for the crest level of 513.5m. In the case of 100% opening for the reservoir level of 540m, the maximum discharge flow is 13200m3/s, equal to the maximum discharge flow over weirs with an upgraded crest level. In other words, the discharge rate in the maximum reservoir level (540m) for the new weir is 16200m3/s or 81% of the PMF discharge over the present weir. On the other hand, the discharge rate for the weir level of 513.5m with a maximum reservoir level of 540m is almost equal to the 5000-year dissipated discharge flow for the same crest level. In other words, this weir cannot pass a 5000-year discharge flow with a reservoir level of 540m. Fig. 31 shows the stage-discharge curve of the weir for the level of 513.5m. The model was implemented again to obtain the discharge flow over the weir with the weir crest at 513.5m and the crest level of 542m. The goal was to determine if the 10000-year control discharge, i.e., the discharge flow of 14000 m^3/s, can pass over the weir with fully open gates or if the flood passes over the weir crest. Table 7 shows the result of this implementation. As shown in this table, the 10000-year discharge flow passes over the weir at the level of 542, i.e., without any freeboard.

Table 7. Pressure over the middle axis of the ogee weir for the crest level of 513.5m and different reservoir levels in the case of the full gate opening

X(m)	-5.20	-1.20	4.40	10.80	16.40	20.40	26.00	30.00	36.40
P (m)	10.63	6.36	3.69	3.66	8.02	13.96	18.59	22.69	29.54

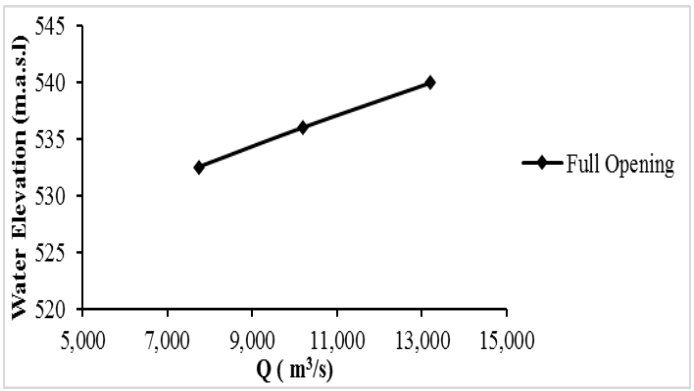

Figure 31. The stage-discharge curve of the weir for the ogee level of 513.5m

The Simulation Results for the Upgraded Weir with the Crest of 513.5m in this section, the averaged velocity and depth are extracted from the numerical model results, and the cavitation index is obtained. The arithmetic means of flow velocity and depth along the weir are used to calculate these parameters transversally. For a fixed value of x, the values of flow depth and velocity for different points are added together and divided by the number of points. It should be noted that according to the results, there are some changes in the depth over the weir opening width. The changes were less significant before the aerator and more significant after it. These changes can be a result of shock waves due to the divergent part of the chute upstream. On the other hand, according to Equation 5, mean depth and velocity are the criteria for calculating the cavitation index. A value for mean depth and velocity should be obtained in each section. It is worth noting that the physical model also reports the transverse depth changes. Table 8 shows the cavitation index for a flood discharge of 3000 m3/s in the case of an upgraded weir for the crest level of 513.5m.

Table 8. The cavitation index with a discharge of 3000 m^3/s over the weir and the chute for the upgraded weir with the crest level of 513.5m

Distance from crest (m)	Fluid depth (m)	Pressure (γ h) (pa)	Depth average velocity (m/s)	Slope	$\frac{V_{ave}^2}{2g}$(m)	$\frac{P_{Abs}}{\gamma} - \frac{P_v}{\gamma}$ (m)	σ
14.25	5.29	51894.9	14.68	27.47	10.98	15.86	1.445
22.25	4.21	41300.1	17.32	31.76	15.29	14.87	0.973
30.25	3.31	32471.1	19.69	25.92	19.76	14.29	0.723
38.25	2.97	29135.7	21.29	20.41	23.10	14.16	0.613
48.09	2.62	25702.2	22.41	13.71	25.61	13.89	0.542
55.95	2.29	22464.9	21.01	8.53	22.49	13.29	0.591
92.00	2.10	20601	23.72	5.00	28.69	12.09	0.421
100.32	2.11	20699.1	23.99	5.14	29.33	11.07	0.377
108.18	2.08	20404.8	24.17	8.75	29.78	11.02	0.370
116.04	2.08	20404.8	24.45	12.52	30.47	10.97	0.360
123.89	2.21	21680.1	23.10	16.44	27.19	11.12	0.409
128.05	2.35	23053.5	23.73	20.51	28.70	11.08	0.386
135.91	2.23	21876.3	23.21	24.61	27.47	11.01	0.401

144.23	1.98	19423.8	26.40	28.90	35.52	10.56	0.297
152.09	1.88	18442.8	27.58	35.00	38.78	10.32	0.266
194.15	2.00	19620	31.00	35.00	48.99	11.64	0.238
220.04	1.85	18148.5	33.40	29.86	56.86	18.61	0.327
227.89	1.40	13734	37.01	13.33	69.82	17.87	0.256
236.21	1.54	15107.4	34.16	-2.12	59.47	17.65	0.297
239.91	1.55	15205.5	33.68	-9.82	57.81	17.50	0.303

Table 9 shows the cavitation index in the case of a 10000-year flood discharge for the ungraded weir with a crest level of 513.5 m.

Table 9. The cavitation index for a 10000-year flood discharge over the weir and chute for the upgraded weir with the crest level of 513.5m

Distance from crest (m)	Fluid depth (m)	Pressure (γ h) (pa)	Depth average velocity (m/s)	Slope	$\frac{V_{ave}^2}{2g}$ (m)	$\frac{P_{Abs}}{\gamma} - \frac{P_v}{\gamma}$ (m)	σ
14.25	19.07	187076.7	18.99	27.47	18.37	33.93	1.847
22.25	17.62	172852.2	19.91	31.76	20.21	32.11	1.589
30.25	15.35	150583.5	20.73	25.92	21.91	30.54	1.394
38.25	13.53	132729.3	22.46	20.41	25.72	29.65	1.153
48.09	11.80	115758	24.03	13.71	29.43	28.40	0.965
55.95	10.83	106242.3	25.22	8.53	32.43	27.73	0.855
92.00	9.22	90448.2	28.10	5.00	40.26	19.19	0.477
100.32	8.98	88093.8	28.93	5.14	42.67	12.56	0.294
108.18	8.81	86426.1	29.50	8.75	44.36	12.19	0.275
116.04	8.95	87799.5	29.67	12.52	44.87	12.04	0.268
123.89	9.10	89271	31.01	16.44	49.00	11.30	0.231
132.21	8.97	87995.7	31.97	22.54	52.10	10.50	0.201
140.07	8.64	84758.4	32.52	26.75	53.91	9.95	0.185
147.93	7.76	76125.6	33.80	31.13	58.22	9.11	0.157
159.95	7.03	68964.3	34.74	35.00	61.50	15.76	0.256
194.15	7.96	78087.6	40.64	35.00	84.18	16.52	0.196
220.04	6.95	68179.5	41.01	29.86	85.71	55.76	0.651
227.89	5.97	58565.7	41.70	13.33	88.62	51.08	0.576
236.21	6.29	61704.9	40.11	-2.12	82.00	50.69	0.618
239.91	6.31	61901.1	39.84	-9.82	80.90	50.24	0.621
243.15	7.05	69160.5	37.43	-14.00	71.42	50.43	0.706

The results show that, similar to the results from the 2D calculations presented in the hydraulic report of the weir of Shahid Abbaspour Dam, the cavitation index decreases for both discharges of 3000 m^3/s and nearly 15000 m^3/s (10000-year discharge) to the 160m station. For the Discharge of 3000 m3/s in the upgraded weir level of 513.5m above sea level and in the 160m station, the cavitation index is obtained to be 0.2 and 0.267 from the 2D and 3D calculations, respectively. After this station upstream, the index decreases in the 2D calculation. With the same Discharge and weir level, the cavitation index also decreases up to 0.238 in the 194m station. After that, it increases again due to reaching the ski-jump bucket and the increase in pressure, which is not considered in the 2D calculations, while the 3D calculations have predicted it. The 3D calculations show a more critical status in the 10000-year Discharge as an index less than 0.2 is seen for the new weir crest level along the chute path. The critical index happens for the weir level of 513.5m

and the 10000-year Discharge in the 135m station. In any case, the cavitation phenomenon is prevented due to the aeration over the chute that occurs after the 124m station. In the 2D calculations of the weir presented in the hydraulic report of Shahid Abbaspour Dam, the pressure seems to be assumed hydrostatically in areas with a steep curve. The concave-up and concave-down flow decrease and increase the pressure, respectively. The following relation is suggested to calculate the pressure in curved areas (h_p) [23].

$$h_p = hcos(\theta) \mp \frac{v^2 h}{gR} \quad (4)$$

V and h are flow velocity and depth in a given point, R is the curve radius at the bottom of the weir, and θ is the slope of a given point to the horizontal axis. In this relation, positive and negative signs are for the concave up and concave down areas, respectively [23]. Khezri et al. demonstrated that this relation provides good results for [24]. Using the 3D calculations and the above relation, the cavitation index is calculated to be 0.77 in the case of a 10000-year discharge and the upgraded weir level of 513.5m above sea level for 52 and 152m stations, while the 2D calculations reported the cavitation index to be 0.554. The 2D calculation reported the cavitation index with a lower value in the 52m station (concave up area) and with a higher value in the 152m stations (concave down area). According to these results, the cavitation index is not critical before the 124m station, which is the first aerating site, and there is no problem with the possible increase of the cavitation if the weir is upgraded. Before implementing the simulations, the numerical model was used for the present weir, and the stage-discharge curve of the weir in various opening degrees, reservoir levels, and pressures over the weir was compared to the available experimental results in different conditions. The difference in the stage-discharge curve is less than 10%, while it is confined to less than 12% in the calculation of the pressures over the weir in most points. The comparisons show that the numerical model obtained the experimental results with good approximation and is reliable. The numerical model was applied for the upgrading plan after it was verified.

4. Conclusion

Large dam reservoir management is changing with increasing water consumption and controlling floods. Changing the conditions of the Shahid Abbaspour Dam basin and the sediments of the dam reservoir, a change in the storage volume of the dam is inevitable. Since the dam weir model is not available and only its report data is available, the use of two-dimensional and three-dimensional flow simulators was considered before building the new physical model.

Flow3D software was used to simulate the dam weir. To accurately investigate the weir, a two-dimensional 80 cm ribbon was constructed from the dam reservoir to the flip bucket. Finally, for a more detailed study, a complete three-dimensional model of the weir was constructed, and the flow conditions on the weir were evaluated. In this simulation, part of the reservoir, weir, transmission channel, aerators, and flip bucket were modeled and validated according to the physical model results and the actual data of the weir. In these conditions, the level of the weir from the sea level is 510, and the flow conditions were controlled by upgrading the overflow to 513.5 meters above sea level. According to the research results in the text of the article, one of the critical cases was the cavitation index and creating negative pressure on the weir in new conditions. Therefore, flow conditions for discharges of 3000 m^3/s and 15000 m^3/s were investigated. The cavitation index is reduced to 160-meters station for both discharges. The cavitation index obtained from two-dimensional calculations for a flow rate of 3000 m^3/s and at an elevated

overflow level of 513.5 meters at a 160-meter station is 0.2 and in three-dimensional calculations is 0.267, and after that Increases again due to reaching the throwing cup and increasing pressure. Three-dimensional calculations showed a more critical situation in the 10,000-year-old discharge, with an index of less than 0.2 for both levels of the weir crown in the index waterway. The critical index occurs at the 513.5 m overflow level and the 10,000-year-old discharge at the 135 m station. Due to aeration on the chute water from the station 124-meters onwards, the air prevents cavitation. According to these results, the cavitation index before the 124-meter station, which is the location of the first aerator, is not critical, and by upgrading the overflow, there is no particular problem in increasing the probability of cavitation.

References

1. Parsaie, A., Shareef, S. J. S., Haghiabi, A. H., Irzooki, R. H. and Khalaf, R. M. 2022. Numerical simulation of flow on circular crested stepped spillway. *Applied Water Science,* 12**,** 1-10.
2. Pirzad, M., Pourmohammadi, M., Ghorbanizadeh Kharazi, H., Solimani Babarsad, M. and Derikvand, E. 2022. Experimental study on flow over arced-plan porous weirs. *Water Supply,* 22**,** 2659-2672.
3. Aein, N., Najarchi, M., Hezaveh, S. M. M., Mehdi NajafiZadeh, M. and Zeighami, E. 2020. Application of 3D Numerical Model and Intelligent Systems in Discharge Coefficient Estimation of Combined Weir-Gate. *Water Resources,* 47**,** 537-549.
4. Yildiz, A., Yarar, A., Kumcu, S. Y. and Marti, A. I. 2020. Numerical and ANFIS modeling of flow over an ogee-crested spillway. *Applied Water Science,* 10**,** 1-10.
5. Rajaa, A. I. and Kamela, A. H. 2020. Performance Study of Fluent-2D and Flow-3D Platforms in the CFD Modeling of a Flow Pattern Over Ogee Spillway. *Anbar Journal for Engineering Sciences,* 8**,** 317-328.
6. Ghazi, B., Daneshfaraz, R. and Jeihouni, E. 2019. Numerical investigation of hydraulic characteristics and prediction of cavitation number in Shahid Madani Dam's Spillway. *Journal of Groundwater Science and Engineering,* 7**,** 323-332.
7. Morovati, K. and Eghbalzadeh, A. 2018. Study of inception point, void fraction and pressure over pooled stepped spillways using Flow-3D. *International Journal of Numerical Methods for Heat & Fluid Flow*.
8. Parsaie, A., Moradinejad, A. and Haghiabi, A. H. 2018. Numerical modeling of flow pattern in spillway approach channel. *Jordan Journal of Civil Engineering,* 12.
9. Daneshfaraz, R., Norouzi, R. and Abbaszadeh, H. 2021. Numerical investigation on effective parameters on hydraulic flows in chimney proportional weirs. *Iranian Journal of Soil and Water Research,* 52**,** 1599-1616.
10. Dehdar-Behbahani, S. and Parsaie, A. 2016. Numerical modeling of flow pattern in dam spillway's guide wall. Case study: Balaroud dam, Iran. *Alexandria Engineering Journal,* 55**,** 467-473.
11. Parsaie, A., Haghiabi, A. H. and Moradinejad, A. 2015. CFD modeling of flow pattern in spillway's approach channel. *Sustainable Water Resources Management,* 1**,** 245-251.
12. Zamiri, E., Karami, H. and Farzin, S. 2020. Studying the effect of shape changes in plan of labyrinth weir on increasing flow discharge coefficient using Flow-3D numerical model. *Irrigation Sciences and Engineering,* 43**,** 101-116.

13. Setyandito, O., Christian, S. and Lopa, R. 2022. Flow Characteristics Investigation On Trapezoidal Weir Using FLOW 3D. *IOP Conference Series: Earth and Environmental Science,* 998**,** 012013.
14. Tajari, M., Dehghani, A. A. and Meftah Halaghi, M. 2021. Semi-analytical solution and numerical simulation of water surface profile along duckbill weir. *ISH Journal of Hydraulic Engineering,* 27**,** 65-72.
15. Shen, Z.-D. and Zhang, Y. 2021. The Three-dimensional Simulation of Granular Mixtures Weir. *IOP Conference Series: Earth and Environmental Science,* 820**,** 012024.
16. Kumar, S., Ahmad, Z. and Mansoor, T. 2011. A new approach to improve the discharging capacity of sharp-crested triangular plan form weirs. Flow measurement and instrumentation*,* 22**,** 175-180.
17. Ghaderi, A., Daneshfaraz, R., Dasineh, M. and Di Francesco, S. 2020. Energy dissipation and hydraulics of flow over trapezoidal–triangular labyrinth weirs. *Water,* 12**,** 1992.
18. Ghanbari, R. and Heidarnejad, M. 2020. Experimental and numerical analysis of flow hydraulics in triangular and rectangular piano key weirs. *Water science,* 34**,** 32-38.
19. Rezazadeh, S., Manafpour, M. and Ebrahimnejadian, H. 2020. Three-Dimensional Simulation of Flow Over Sharp-Crested Weirs Using Volume of Fluid Method. *Journal of Applied Engineering Sciences,* 10.
20. Fuentes-Pérez, J. F., Quaresma, A. L., Pinheiro, A. and Sanz-Ronda, F. J. 2022. OpenFOAM vs FLOW-3D: A comparative study of vertical slot fishway modelling. *Ecological Engineering,* 174**,** 106446.
21. Hager, W. H. 2010. Wastewater hydraulics: Theory and practice.
22. Kim, D. G. and Park, J. H. 2005. Analysis of flow structure over ogee-spillway in consideration of scale and roughness effects by using CFD model. *KSCE Journal of Civil Engineering,* 9**,** 161-169.
23. Singh, V. P. Ven Te Chow: An Outstanding Scholar. World Environmental and Water Resources Congress 2014, 2014. 753-763.
24. Khezri, N., Zarrati, A. R. and Golzari, F. 2009. Calculation of Pressure Distribution over Flip Buckets. *Journal of Hydraulics,* 3**,** 39-52.

© 2022 by the authors. Licensee SCU, Ahvaz, Iran. This article is an open access article distributed under the terms and conditions of the Creative Commons Attribution 4.0 International (CC BY 4.0 license) (http://creativecommons.org/licenses/by/4.0/).